ORGANIC PROCESS RESEARCH & DEVELOPMENT
OPR&D
Article
pubs.acs.org/OPRD

# First Study of the Thermal and Storage Stability of Arenediazonium Triflates Comparing to 4-Nitrobenzenediazonium Tosylate and Tetrafluoroborate by Calorimetric Methods

Alexander A. Bondarev,*[,†] Evgeny V. Naumov,[†] Assiya Zh. Kassanova,[‡] Elena A. Krasnokutskaya,[§] Ksenia S. Stankevich,[§] and Victor D. Filimonov*[,§]

[†]Department of Biomedicine, Altai State University, Barnaul 656049, Russian Federation
[‡]S. Toraighyrov Pavlodar State University, Pavlodar 140000, Kazakhstan
[§]The Kizhner Research Center, National ResearchTomsk Polytechnic University, Tomsk 634050, Russian Federation

Supporting Information

**ABSTRACT:** Herein, for the first time, using isothermal flow calorimetry and differential scanning calorimetry (DSC)/thermal gravimetric analysis (TGA), we have determined the thermal decomposition energies for the number of solid arenediazonium triflates comparing to 4-nitrobenzene tosylate and 4-nitrobenzentetrafluoroborate. The kinetics of thermal decomposition, activation energies, and half-lives of the studied diazonium salts (DSs) were found. Using gas chromatography−mass spectrometry (MS) and liquid chromatography−MS, we have elucidated the products formed during thermolysis of the investigated DSs. By density functional theory quantum chemical calculations at the B3LYP/aug-cc-pVDZ level of theory, we simulated the thermodynamics of decomposition reactions proceeding via substitution of the diazonium group by corresponding nucleophiles. The method applied predicted the decomposition energies of all the studied compounds fairly precise, except for 2-nitrobenzene diazonium triflate. It has been found that 4-nitrobenzene diazonium triflate has increased storage stability under normal conditions comparing to the corresponding tosylate and tetrafluoroborate. The experimental and theoretical results demonstrated that comparing to DSC/TGA, isothermal flow calorimetry more adequately reflects the energetics of the thermal decomposition of DSs and their storage stability under normal conditions.

**KEYWORDS:** *arenediazonium salts, stability, isothermal flow calorimetry, quantum chemical calculation, thermolysis*

## INTRODUCTION

Aromatic diazonium salts (DSs) are versatile synthetic blocks widely used in fine organic synthesis and industry.[1] Beyond that, DSs have been increasingly applied in development of macro- and nanoscale composite materials because of their reactivity toward metal and nonmetal surfaces.[2a]

Nevertheless, such disadvantages as a poor storage stability in the solid state and a propensity to explosive decomposition upon heating, photo-irradiation, or mechanical stress limit the preparation and usage of DSs, especially, on an industrial scale.[1a,2b−d] Several approaches to the stabilization of hazardous DSs, allowing for the minimization of risks associated with the processes of their production and utilization, are available. These include, for instance, preparation of polymer-supported DSs,[2e] freezing of benzenediazonium chlorides up to −84 °C,[2f] and application of flow chemistry techniques for DS chemistry.[2g] Besides, to diminish the hazard level of DSs, twelve rules of handling these compounds were formulated.[2b]

Recently, we have synthesized arenediazonium tosylates $ArN_2^+TsO^-$ (ADTs)[3a] and trifluoromethane sulfonates $ArN_2^+TfO^-$ (ADTfs)[3b] that showed major advantages over traditional DSs. While being surprisingly stable in the solid state, they retained high reactivity in a vast array of diazonium chemistry reactions including the formation of aromatic iodides and bromides,[3a,b,4a−f] azides[3b,4g] and boronic acids,[3b] and Pd-catalyzed C−C-cross-compling.[3b,4h−j] Additionally, it has been shown that ADTs can be successfully used for introducing the $^{19}F$ isotope into the aromatic ring,[5a] carrying out azo-coupling with ethyl−methyl acetoacetate,[5b] substituting the diazonium group with the triethoxysilyl moiety,[5c] and covalently grafting aromatic groups to carbonized metal nanoparticles[5d] and graphene.[5e]

The thermal decomposition energies of some ADTs and ADTfs determined by differential scanning calorimetry (DSC)/thermal gravimetric analysis (TGA), in most cases were found to be below 800 J/g.[3a,b,4g] Therefore, according to the safety criteria of the United Nations Economic Commission for Europe (UNECE), they can be referred as compounds that can be transported safely.[6] However, the products of their thermal decomposition have not been studied and remain unknown. Moreover, DSC/TGA provides information about thermal decomposition energy at increased temperatures and does not reflect decomposition processes taking place under normal conditions. To comprehensively assess the possibility of safe use of ADTs and ADTfs in the laboratory and on an industrial scale, it is necessary to determine reliable quantitative characteristics of their storage stability in a solid state and thermal decomposition energies.

**Received:** July 3, 2019
**Published:** September 13, 2019





DOI: 10.1021/acs.oprd.9b00307
Org. Process Res. Dev. XXXX, XXX, XXX−XXX

Such evaluations should be performed using various methods and comparing to other types of DSs.

Noteworthy, the DS decomposition in solution has been extensively investigated for a long time (see, e.g., refs[1a,g]), whereas not many studies cover stability and safety of DSs in the solid state. The paucity of quantitative data, describing the decomposition of solid DSs, reflects the lack of reliable generally accepted procedures for measuring the above-mentioned properties.

A comparative study of the stability of the solid DSs (chlorides, tetrachlorozincates and tetrafluoroborates) was reported in,[7a,c] however, the decomposition products were not given. The investigation of the thermal decomposition of $^{14}$N- and $^{15}$N-substituted arenediazonium chlorides and tetrafluoroborates has shown that the isotope effect is insensitive to the nature and position of substituents in the aromatic ring and the nature of the counterion.[7b] The stability test of arenediazonium chlorides has demonstrated that the sensitivity to detonation decreases from ortho-, through meta-, to para-substitution.[7a] It was shown that the nature of the substituent in the aromatic nucleus has a pronounced effect on DS stability as the nitro derivatives were significantly more sensitive to impact than the chlorine derivatives. The decrease in detonation sensitivity with an increase in molecular weight was observed, which was associated with a decrease in the specific value of the energy released per unit mass. The authors noted that the detonation sensitivity of DSs depends on many factors such as the size and shape of the crystals, as well as the presence of impurities. No correlation between detonation sensitivity and thermal stability was found.[7a] The values of the thermal decomposition energies of some ADTs and ADTfs, determined by DSC/TGA, do not correlate with the structural features of the diazonium cation or the nature of counterion.[3a,b,4g] The commonly occurred term "the storage stability of DS" has not yet been described quantitatively. To address this issue, in most cases the ability of DSs to be stored without changes for a certain time is indicated. Besides, to the best of our knowledge, up to the present, there are no theoretical methods for predicting the energies of thermal decomposition of DSs based on their chemical structure.

Our work aims to comprehensively address the challenges associated with the thermal and storage stability assessment of DSs. To achieve that, we for the first time have studied the kinetics and thermodynamics of thermal decomposition of arenediazonium triflates **1a−d** comparing to 4-nitrobenzenediazonium tosylate **2** and tetrafluoroborate **3** by DSC/TGA and isothermal flow calorimetry. Additionally, we have endeavored to develop the criteria for the evaluation of the storage stability of an array of DSs with various counterions and substituents. The electron-withdrawing nitro group and the electron-donating methoxy group were chosen as substituents in the aromatic core of ADTfs **1a−d** for the following reasons. First, according to,[7a] DSs with $NO_2$-moieties are the most explosive, therefore they represent the highest threshold of these properties. Second, DSs with $NO_2$- and MeO-substituents in the aromatic ring differ sharply in their properties,[3a,b] that is these two examples should cover the widest range of properties studied.

We also aimed to determine the possibility to apply density functional theory (DFT) quantum chemical calculations for the theoretical evaluation of the DS thermal decomposition and clarification of its mechanism. To the best of our knowledge, DFT methods have not been previously used for these purposes. To investigate the mechanism, a gas chromatography (GC)−mass spectrometry (MS) and liquid chromatography (LC)−MS study of the decomposition products of DSs **1a−d**, **2**, **3** was carried out. The obtained results are valuable for both applied and theoretical field of diazonium chemistry. On the one hand, they allow assessing the stability, capabilities, and limitations of DSs for industrial use. On the other hand, they provide better understanding of the mechanisms of DS thermal decomposition and allow to establish the structure−stability relationship.

## EXPERIMENTAL SECTION

Arenediazonium triflates **1a−d** and 4-nitrobenzenediazonium tosylate **2** were synthesized according to the procedure described previously.[3a,b] 4-Nitrobenzenediazonium tetrafluoroborate **3** was purchased from Aldrich (CAS no. 456-27-9). All samples used in calorimetric studies were dried in vacuum for 48 h. This procedure is recommended in the study of the decomposition of arendiazonium chlorides.[7a]

The DSC/TGA runs were made in argon atmosphere using open sample pans on Q600 SDT instrument (TA Instruments), a heating rate of 5 °C·min$^{-1}$, and a temperature range of 20−600 °C. A typical sample size was 10 mg.

Heat flow was measured under isothermal conditions in the nitrogen atmosphere using TAM III microcalorimeter (TA Instruments). The experiments were conducted according to the conventional approach that is used for calorimetric studies of the safety of high-energy materials.[8] The sample was put in a glass beaker placed in a standard calorimeter ampoule made from Hastelloy with a volume of 1 mL. The ampoule was evacuated, then purged with nitrogen, argon, or air depending on experimental conditions and sealed. The heat flow was measured at three different temperatures: 75, 80, and 85 °C. We conducted all flow calorimetry experiments at temperatures significantly lower than the melting points in order to adequately approximate kinetic curves to normal conditions. The isothermal test was carried out until the heat flux decreased below 2 $\mu$W. This value is less than 1% of the maximum heat flux and corresponds to the conversion degree $\alpha > 0.99$. Time was varied from 1 to 50 days depending on sample and temperature. The acquired experimental curves were approximated using the model of an autocatalytic process and the Arrhenius equation. The experimental data were processed using TAM Assistant Software v1.3.0.153. Gnuplot 4.5[9a] and R Statistics v3.3.3[9b] were used for mathematical processing, statistical analysis, and dependencies building.

The DS decomposition products were studied by GC−MS on an Agilent 7890A/5975C instrument. The typical sample size was 50 mg. Samples were heated in a thermostat at 85 °C for 14 days. Then an aqueous solution of KI was added to the sample to convert the undecomposed DSs into the corresponding volatile aryl iodides,[3a,b] the products were extracted with ethyl acetate and organic layer was filtered through a silica pad. The obtained ethyl acetate extracts were then analyzed by GC−MS.

All LC−MS experiments were carried out on a high-resolution time-of-flight mass spectrometer Agilent LC-1260 MS QTOF 6530 equipped with electrospray ionization source (ESI) and atmospheric pressure chemical ionization source (APCI). A chromatographic method was developed using a ZORBAX Eclipse Plus column (C18, 2.1 × 50 mm, 1.8 $\mu$m). The following gradient elution with water as "A" and acetonitrile as "B" was used at a flow rate of 0.25 mL/min:


DOI: 10.1021/acs.oprd.9b00307
Org. Process Res. Dev. XXXX, XXX, XXX−XXX

0–40 min, 0% B → 100% B followed by isocratic elution with B for 20 min. The operating parameters of the ESI-QTOF-MS were: gas flow rate, 9 L/min ($N_2$); drying gas temperature, 350 °C; nebulizer, 35 psi; sheath gas flow, 11 L/min; sheath gas temperature, 300 °C, capillary, 3500 V; skimmer, 65 V; octopole radio frequency (rf) voltage, 750 V; fragmentor 150 V; and energy of collision 20 eV. The operating parameters of the APCI-TOF-MS were: gas flow rate, 6 L/min ($N_2$); drying gas temperature, 300 °C; nebulizer, 35 psi; vaporizer temperature, 400 °C; capillary, 3500 V; skimmer, 65 V; octopole rf voltage, 750 V; fragmentor, 150 V; and energy of collision 20 eV. For the LC–MS experiments, the DS decomposition products were dissolved in a water/acetonitrile mixture (1:1 v/v) at a concentration of 1 mg/mL. The volume of the sample injected was 5 $\mu$L. Acquired LC–MS spectra were processed using the OpenMS 2.0 software package.[10]

For the theoretical study of suggested DS decomposition routes, the quantum-chemical calculations were performed using Kohn–Sham DFT, global-hybrid GGA functional B3LYP, and aug-cc-pVDZ basis set in Gaussian 09 software package.[11] At the first step, the geometry of all molecules participating in the reactions was optimized. To prove the nature of the stationary points, the harmonic frequency calculations were performed. Thereafter, the vibrational frequencies and thermodynamic corrections were calculated at normal conditions (25 °C, 1 atm) and at temperatures used for isothermal decomposition experiment (75, 80, and 85 °C).

## RESULTS AND DISCUSSION

**DSC/TGA Results.** Our study of the thermal and storage stability of arenediazonium triflates **1a–d**, 4-nitrobenzenediazonium tosylate **2** and tetrafluoroborate **3** has begun from collecting DSC/TGA data. Figures 1–6 show DSC/TGA

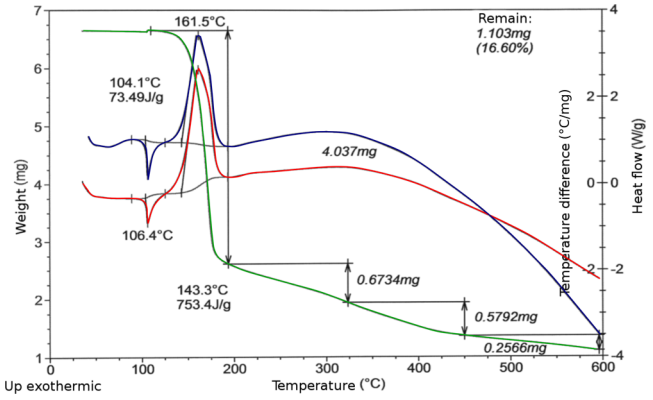


**Figure 1.** DSC/TGA thermograms of thermal decomposition of 2-$NO_2C_6H_4N_2^+TfO^-$ **1a**. The temperature difference is shown in red; the sample weight is shown in green; the heat flow is shown in blue.

curves of thermal decomposition of DSs **1–3**. It can be seen that upon heating all the investigated DSs decompose with energy and weight loss. The temperatures and decomposition energies are summarized in Table 1.

For the DSs **1a**, **1b**, **1d**, **3** additional low-temperature endothermic effects are observed in the temperature range close to their melting point, whereas DSs **1c**, **2** decomposed only exothermically (Figures 1–6, Table 1). Note that DS **2** decompose giving two exothermic peaks (Figure 5). The first one at 69.37 °C is characterized by a small amount of heat released (24.47 J/g) and can be caused by the baseline issue, or

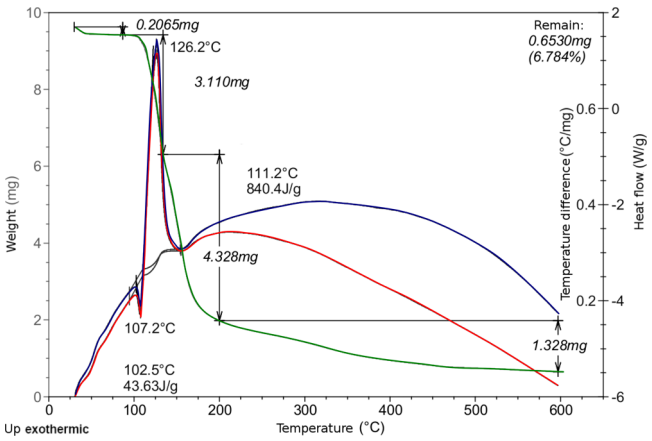


**Figure 2.** DSC/TGA thermograms of thermal decomposition of 3-$NO_2C_6H_4N_2^+TfO^-$ **1b**. The temperature difference is shown in red; the sample weight is shown in green; the heat flow is shown in blue.

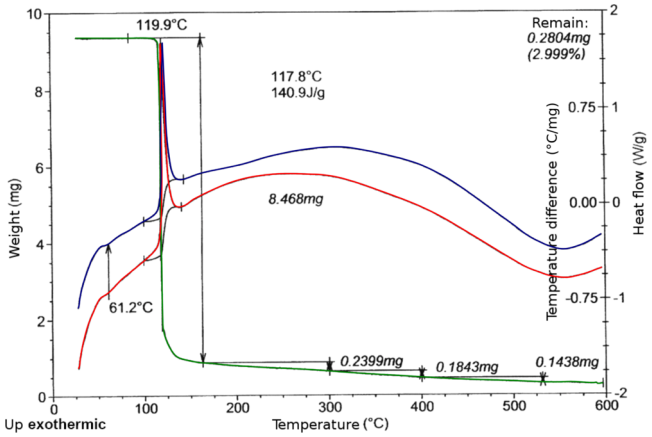


**Figure 3.** DSC/TGA thermograms of thermal decomposition of 4-$NO_2C_6H_4N_2^+TfO^-$ **1c**. The temperature difference is shown in red; the sample weight is shown in green; the heat flow is shown in blue.

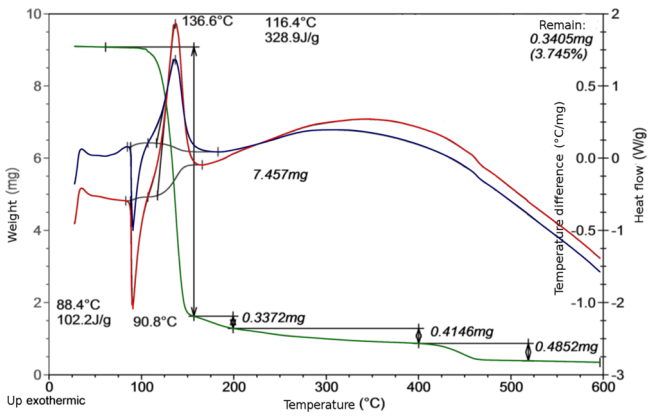


**Figure 4.** DSC/TGA thermograms of thermal decomposition of 4-$MeOC_6H_4N_2^+TfO^-$ **1d**. The temperature difference is shown in red; the sample weight is shown in green; the heat flow is shown in blue.

crystallization from the amorphous phase. While for the second one, located at 146.6 °C, the heat release of 323.0 J/g is observed. In the case of DSs **1a**, **1b**, **1d** the endothermic peaks are not accompanied by a weight loss and are probably associated with the rearrangement of the crystal lattice.



DOI: 10.1021/acs.oprd.9b00307
Org. Process Res. Dev. XXXX, XXX, XXX–XXX

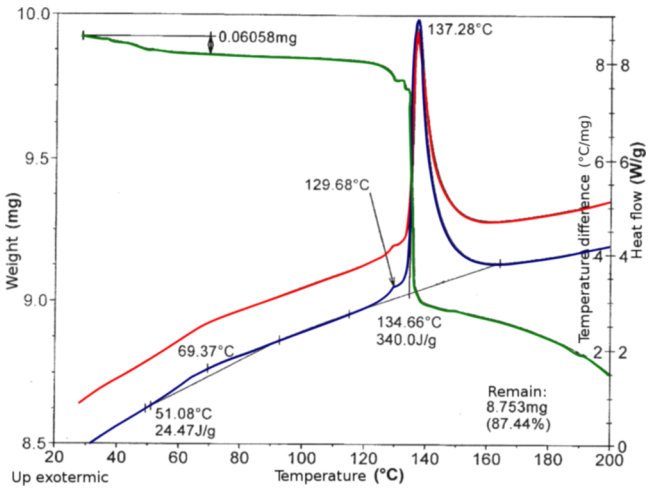


**Figure 5.** DSC/TGA thermograms of thermal decomposition of 4-$NO_2C_6H_4N_2^+TsO^-$ **2**. The temperature difference is shown in red; the sample weight is shown in green; the heat flow is shown in blue.

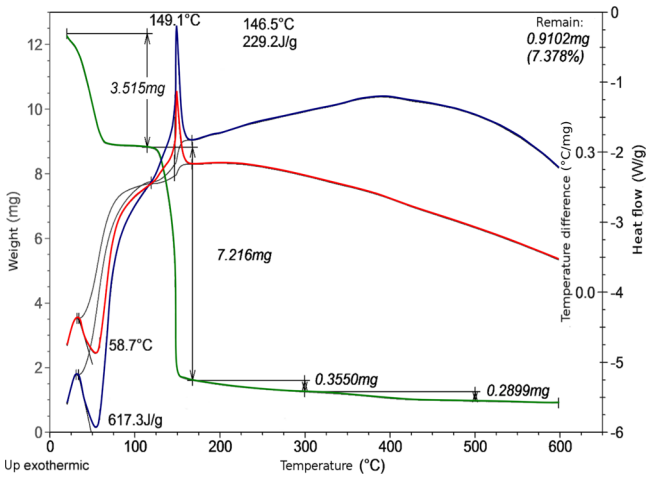


**Figure 6.** DSC/TGA thermograms of thermal decomposition of 4-$NO_2C_6H_4N_2^+BF_4^-$ **3**. The temperature difference is shown in red; the sample weight is shown in green; the heat flow is shown in blue.

The weight loss upon heating DS **3** in the endothermic process, starting at 58.7 °C is 28.5%, which corresponds exactly to the elimination of volatile $BF_3$ (28.6%) according to reaction 1

$$\underset{\mathbf{3}}{4\text{-}NO_2C_6H_4N_2^+BF_4^-} \rightarrow \underset{\mathbf{3a}}{4\text{-}NO_2C_6H_4N_2^+F^-} + BF_3 \quad (1)$$

It might seem that the loss of $BF_3$ at 58.7 °C indicates that intermediate **3a** undergoes decomposition at 146.5 °C (eq 1). However, upon thermal decomposition of $PhN_2^+BF_4^-$, a small endothermic peak at 63 °C was also observed on the DSC/TGA curves. The appearance of this peak was explained by the removal of water bound to DS via hydrogen bonds.[12] It cannot be applied to DS **3** , as the weight loss of DS **3** at 58.7 °C corresponds to 5.2 mol of water per 1 mol of DS **3**. Should it be such a large amount of water, DS **3** would have to be partially dissolved, but not crystalline. Hence, there are contradictions in explaining the cause of the endothermic peak appearance during the heating of DS **3** and $PhN_2^+BF_4^-$. Obviously, this issue requires further special studies. Therefore, at present, we can propose eq 1 only as a hypothesis, partially consistent with the results of quantum-chemical modeling of DS decomposition reactions.

The major weight loss upon heating of DSs **1**−**3** occurs in exothermic processes, which are clearly associated with the formation of volatile decomposition products (Figures 1−6).

The exothermic effects $\Delta H_{exoterm}$ of DSs **1**−**3** thermal decomposition are the most important for the DS safety evaluation. As can be seen from Table 1, these effects strongly depend on the nature and position of the substituent in the benzene ring and partly on the nature of counterions. Among salts **1a**−**d** with a triflate counterion, the energy release during decomposition is the highest for 3-nitro-derivative **1b** and

**Table 2. Reproducibility of the DS 2 Thermal Decomposition Parameters Measured at 85 °C Depending on Synthetic Batch and a Number of Reprecipitations**[a]

| sample | $k\cdot10^3$, $s^{-1}$ | $\Delta H$, kJ/mol | $P_0$, mW/g |
|---|---|---|---|
| sample 1 nitrogen (reprecipitation 1) | 0.2723 ± 0.0364 | 234.2 ± 3.0 | 31.2 ± 8.1 |
| sample 2 nitrogen, (source, reprecipitation 1) | 0.2568 ± 0.0371 | 243.6 ± 20.7 | 12.7 ± 3.5 |
| sample 3 nitrogen, (source, reprecipitation 1) | 0.2639 ± 0.0283 | 235.5 ± 7.0 | 10.1 ± 3.5 |
| sample 3 air, reprecipitation 2 | 0.2683 ± 0.0333 | 229.0 ± 28.9 | 8.7 ± 8.5 |
| sample 3 argon, reprecipitation 2 | 0.3119 ± 0.0352 | 242.3 ± 8.0 | 12.8 ± 2.4 |
| sample 2, 3 nitrogen, (source, reprecipitation 1, 2) | 0.2608 ± 0.0184 | 238.9 ± 7.8 | 11.2 ± 2.3 |
| sample 4 nitrogen, source | 0.2589 ± 0.0340 | 241.7 ± 16.2 | 12.0 ± 2.0 |
| sample 4 nitrogen, reprecipitation 1 | 0.2608 ± 0.0492 | 235.1 ± 17.9 | 10.2 ± 6.3 |
| sample 4 nitrogen, reprecipitation 2 | 0.2898 ± 0.0221 | 238.1 ± 6.8 | 11.3 ± 2.3 |
| general statistics | 0.2745 ± 0.0140 | 237.7 ± 4.6 | 13.8 ± 3.3 |

[a]$k$—rate constant, $\Delta H$—integral enthalpy, $P_0$—initial heat flow.

**Table 1. Temperatures and Decomposition Energies of Diazonium Salts 1−3 According to DSC/TGA Experiments Data**

| | endothermic process | | exothermic process | | |
|---|---|---|---|---|---|
| DSs | $T$, °C | $\Delta H$, J/g (kJ/mol) | $T$, °C | $\Delta H$, J/g (kJ/mol) | $M_p$, °C |
| 2-$NO_2C_6H_4N_2^+TfO^-$ **1a** | 104.1 | 73.49 (21.98) | 143.3 | −753.4 (−225.3) | 110 |
| 3-$NO_2C_6H_4N_2^+TfO^-$ **1b** | 102.5 | 43.6 (10.04) | 111.2 | −840.4 (−251.3) | 108−109 |
| 4-$NO_2C_6H_4N_2^+TfO^-$ **1c** | | | 116.4 | −219.9 (−65.7) | 104 |
| 4-$MeOC_6H_4N_2^+TfO^-$ **1d** | 88.4 | 102.2 (29.05) | 136.6 | −328.9 (−93.5) | 94−97 |
| 4-$NO_2C_6H_4N_2^+TsO^-$ **2** | | | 69.37 | −24.47 (−7.8) | 132 |
| | | | 146.6 | −323.0 (−103.7) | |
| 4-$NO_2C_6H_4N_2^+$ $BF_4^-$ **3** | 58.7 | | 146.5 | −229.2 (−54.3) | 144 |



DOI: 10.1021/acs.oprd.9b00307
Org. Process Res. Dev. XXXX, XXX, XXX−XXX

Table 3. Integral Enthalpy and Maximum Heat Flow Values Found during Isothermal Decomposition of Diazonium Salts 1−3[a]

| DS | $\Delta H$, kJ/mol | | | $P_{max}$, mW/g | | |
|---|---|---|---|---|---|---|
| | 75 °C | 80 °C | 85 °C | 75 °C | 80 °C | 85 °C |
| 2-$NO_2C_6H_4N_2^+TfO^-$ (**1a**) | 414.0 | 386.0 | 396.0 | 0.705 | 1.49 | 2.33 |
| 3-$NO_2C_6H_4N_2^+TfO^-$ (**1b**) | 227.9 | 230.0 | 225.4 | 6.57 | 14.15 | 28.8 |
| 4-$NO_2C_6H_4N_2^+TfO^-$ (**1c**) | 200.0 | 235.1 | 250.0 | 20.12 | 47.89 | 119.5 |
| 4-$MeOC_6H_4N_2^+TfO^-$ (**1d**) | 183.1 | 183.2 | 106.0 | 1.34 | 2.97 | 5.37 |
| 4-$NO_2C_6H_4N_2^+TsO^-$ (**2**) | 253.0 | 232.4 | 231.0 | 21.10 | 34.82 | 64.60 |
| 4-$NO_2C_6H_4N_2^+$ $BF_4^-$ (**3**) | 173.0 | 156.0 | 147.0 | 20.02 | 31.63 | 66.87 |

[a]$\Delta H$—integral enthalpy, $P_{max}$—maximum heat flow value.

decreases noticeably in the row **1b** > **1a** > **1d** > **1c**. Among DSs having the same 4-nitrobenzene diazonium cation and different counterions, the energy release decreases in the row **2c** > **1c** ≈ **3**. Therefore, the highest heat release is observed for DS with a TsO-counterion. However, a change in the counterion nature affects the exothermic decomposition process substantially less than the position and type of substituents in the benzene ring.

**Isothermal Flow Calorimetry Results.** With DSC/TGA data in our hands, we moved on to isothermal flow calorimetry analysis of DSs studied. As the stability of DS could be affected by the presence of impurities, which often cannot be controlled by conventional analytical methods,[1a,7a] we first decided to evaluate the reproducibility of thermal decomposition parameters measured. To do that we took samples of ADTS **2** from three synthetic batches obtained under identical conditions (samples 1−3) and samples of ADTS **2** purified by single and double precipitation of sample **3** from acetic acid/ether solutions (repricipitation 1 and 2). During the isothermal decomposition, the following parameters have been determined: the integral enthalpy, initial and maximum heat flows, decomposition rate constants, and initial product concentrations approximated by eq 2. Additionally, we have varied the purged gas and studied sample decomposition in air, argon, and nitrogen atmosphere. The results show that the collected data are consistent, and the results do not depend statistically significantly on the degree of sample purification. Even though there is a slight tendency to the reduction of the initial heat flow depending on the number of reprecipitations, the differences between the first and second reprecipitation are minimal. No qualitative and statistically significant differences were observed when decomposition was conducted in air, argon, and nitrogen atmosphere. The average statistical deviation (RMD) for the rate constants (according to eq 2) and the enthalpy was 5%. Therefore, the further isothermal flow calorimetry experiments were carried out in a nitrogen atmosphere and after a single reprecipitation of the initial DS.

Table 3 and Figures 7−10 show the results of isothermal decomposition of DSs **1**−**3** at 75, 80, and 85 °C. At 75 °C, the maximum heat flow values obtained for the 4-nitrobenzene DSs **1c**, **2**, **3** almost do not depend on the counterion nature. However, it can be noted that the heat flow curve acquired during DS **1c** decomposition is much steeper. Additionally, the $P_{max}$ values obtained for this DS at 80 and 85 °C are significantly higher than those for DS **2** and **3**. The $P_{max}$ values found for 4-methoxybenzenediazonium triflate **1d** are noticeably smaller compared to 4-nitrobenzenediazonium triflate **1c**. Among the nitrobenzenediazonium triflates **1a**−**c**, the maximum heat flow decreases from *para*-**1c**, through *meta*-**1b**, to *ortho*-**1a** substitution. The values of $P_{max}$ are important not only for mathematical modeling of the reaction kinetics but also for quantitative description of the compound safety that is essential for practical application.

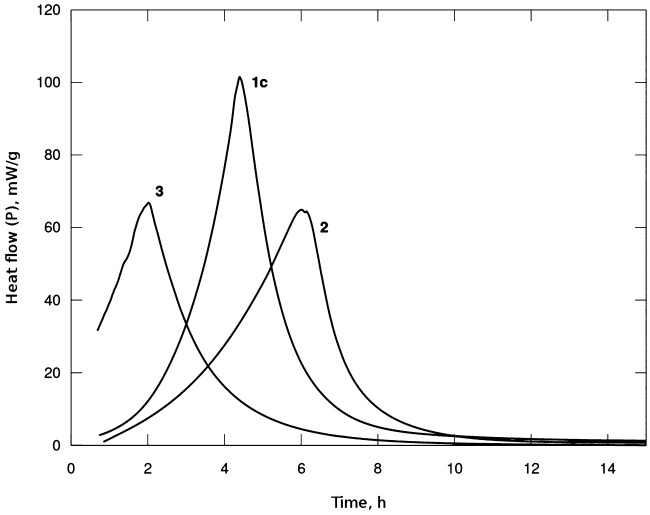


**Figure 7.** Heat flow ($P$) during isothermal decomposition of nitrobenzenediazonium salts: tetrafluoroborate **3**, tosylate **2**, and triflate **1c** at 85 °C.

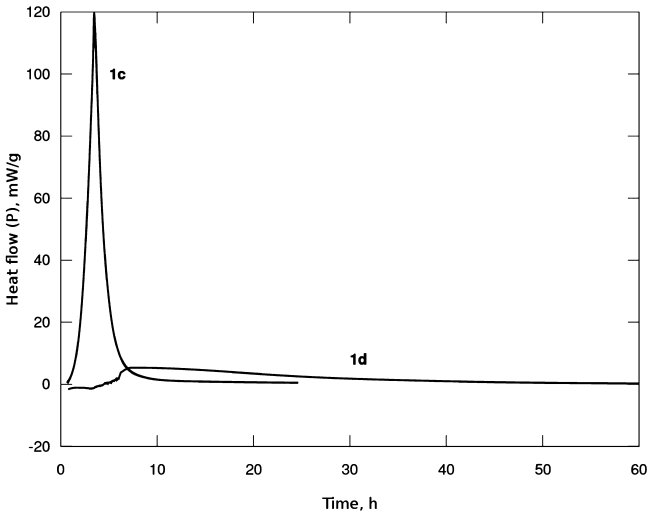


**Figure 8.** Heat flow ($P$) during isothermal decomposition of 4-nitrobenzenediazonium **1c** and 4-methoxybenzenediazonium **1d** triflates at 85 °C.

To investigate the kinetics of isothermal decomposition (Figures 7−10), we approximated the experimental heat flow curves with kinetic equation for autocatalytic reaction 2 that qualitatively describes the heat flow over time dependency.



DOI: 10.1021/acs.oprd.9b00307
Org. Process Res. Dev. XXXX, XXX, XXX−XXX

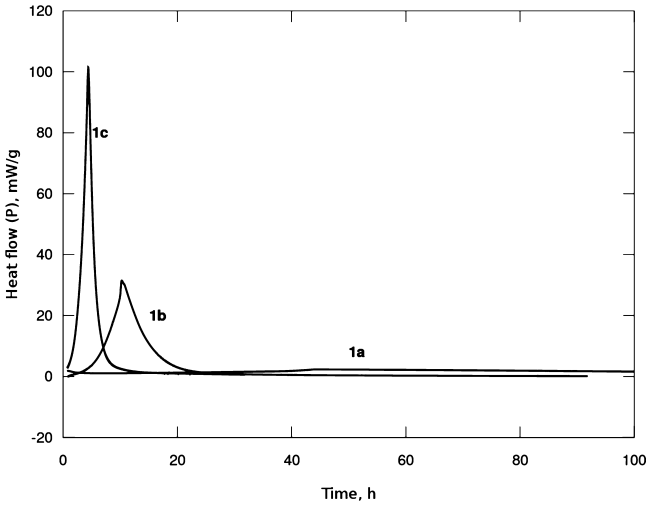


**Figure 9.** Heat flow ($P$) during isothermal decomposition of 2-, 3- and 4-nitrobenzenediazonium triflates **1a–c** at 85 °C.

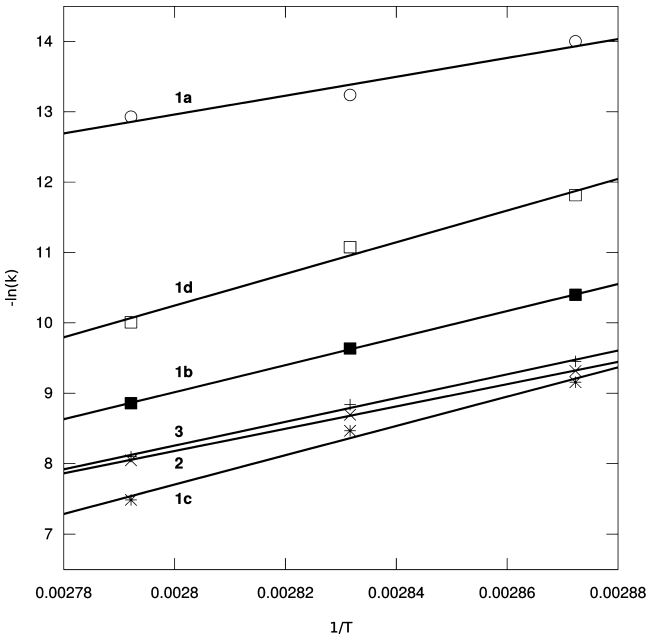


**Figure 10.** Results of the approximation of DS **1–3** decomposition reactions with the Arrhenius equation.

The following main parameters were determined: $k$—rate constant, and $P_0$, $P_{max}$—values of the initial and maximum heat flows in the autocatalytic reaction eq 2. Table 4 shows calculated kinetic parameters found as a result of approximation of the experimental heat flow curves of DSs **1a–1d**, **2**, **3**. The following kinetic equation describing autocatalytic reaction was applied: $aA \rightarrow cC$

$$\frac{d\alpha}{dt} = k(T)\cdot f(\alpha) \quad (2)$$

$$\alpha = \frac{A_0 - A}{A_0} = \frac{a}{c}\cdot\frac{C}{A_0} \quad (3)$$

$$f(\alpha) = a^m\cdot(1-\alpha)^n = \alpha\cdot(1-\alpha) \quad (4)$$

$$k(T) = B\cdot e^{-E_a/RT} \quad (5)$$

$$P = k(T)\cdot\alpha\cdot(1-\alpha)\cdot A_0\cdot\Delta H \quad (6)$$

where $\alpha$—conversion degree; $k(T)$—rate constant, [$s^{-1}$]; $f(\alpha)$—the kinetic model in differential form; $A_0$, $A$—initial and current concentration of DS, which for solid-phase reactions are measured in mol/g units; $C_0$, $C$—initial and current concentrations of products, [mol/g]; $a$, $c$—stoichiometric coefficients, for the processes studied $a/c = 1$; $P$, $P_0$—current and initial heat flow; $\Delta H$—reaction enthalpy; $B$—is the pre-exponential factor, a constant for each chemical reaction; $E_a$—an experimentally determined parameter that indicates the sensitivity of the reaction rate to temperature; $R$—the universal gas constant (8.315 J·$K^{-1}$·$mol^{-1}$); $T$—the absolute temperature (in K).

The kinetic eq 2 is used to model solid-phase reactions,[13,14] and can be expressed in terms of the conversion degree $\alpha$ (eq 3). The kinetic curves for the reactions studied are best described by eq 4 at $m = 1$ and $n = 1$. The temperature dependence of the reaction rate is expressed by the Arrhenius eq 5. The reaction enthalpy $\Delta H$ is calculated by integrating a curve approximating the experimental heat flux (eq 6), in the time interval (0, ∞). The half-life corresponds to the conversion degree of 0.5. Because of the symmetry of the approximating kinetic curve 4, the half-life coincides with the maximum heat flux (in the case of more complex kinetics, this rule is not fulfilled).

Figure 7 shows the experimental heat flow curves describing the isothermal decomposition of DSs **1c**, **2** and **3** at 85 °C. As can be seen, the half-life of DSs depends on the counterion: for tetrafluoroborate **3** it is 2 h, for triflate **1c**—4 h, and for tosylate **2**—6 h.

The experimental heat flow curves describing the isothermal decomposition of salt **1a** are more complex and, therefore, differ from the curve characteristic for the autocatalytic process. At the initial stage, a decrease in the heat flow is observed, which is associated with a higher rate of the endothermic process. Then, the heat flow is increased

**Table 4. Kinetic Parameters of the Isothermal Decomposition of DSs 1–3 ($P_0$—Initial Heat Flow Value, $k$—Rate Constant Calculated According to the eq 2)**

| | $P_0$, mW/g | | | $k\cdot10^3$, $s^{-1}$ | | |
|---|---|---|---|---|---|---|
| DS | 75 °C | 80 °C | 85 °C | 75 °C | 80 °C | 85 °C |
| 2-$NO_2C_6H_4N_2^+TfO^-$ **1a** | 40.6 | 88.2 | 147.0 | 0.00087 | 0.00184 | 0.00254 |
| 3-$NO_2C_6H_4N_2^+TfO^-$ **1b** | 0.94 | 11.0 | 44.6 | 0.03048 | 0.06545 | 0.14339 |
| 4-$NO_2C_6H_4N_2^+TfO^-$ **1c** | 9.0 | 13.1 | 48.4 | 0.10562 | 0.21057 | 0.53446 |
| 4-$MeOC_6H_4N_2^+TfO^-$ **1d** | 14.78 | 32.00 | 113.8 | 0.00739 | 0.01548 | 0.04504 |
| 4-$NO_2C_6H_4N_2^+TsO^-$ **2** | 19.57 | 27.5 | 41.5 | 0.08995 | 0.16775 | 0.32057 |
| 4-$NO_2C_6H_4N_2^+BF_4^-$ **3** | 392.4 | 896.0 | 1804.2 | 0.07851 | 0.14520 | 0.30432 |



DOI: 10.1021/acs.oprd.9b00307
Org. Process Res. Dev. XXXX, XXX, XXX–XXX

indicating the predominance of the exothermic process. The presence of the endothermic process is consistent with the DSC/TGA data (Table 1). To describe the kinetics of these reactions, we used the model of two sequential and two parallel autocatalytic processes. The deconvolution results are given in detail in Supporting Information 1s. Table 4 shows the parameters of the heat flow kinetics calculated when isothermal decomposition reaction is approximated by a single autocatalytic process corresponding to the main exothermic stage. This stage is the most important as it determines the main characteristics of safety and stability of DSs.

The half-life of 4-nitrophenyldiazonium triflate **1c** is significantly less than the half-life of 4-methoxyphenyldiazonium triflate **1d**: the values found are 4 and 16 h, respectively. At the same time, the heat flow observed during decomposition of 4-nitrophenyldiazonium triflate **1c** is much higher than that of 4-methoxyphenyldiazonium triflate **1d** (Figure 8): 119.5 mW/g for **1c** versus 5.37 mW/g for **1d** (Figure 8).

The substitution pattern in the aromatic ring has a pronounced effect on the DS stability. Among DS with triflate counterion, the longest half-life time at 85 °C has ortho-derivative **1a** (62 h). The meta-derivative **1b** is less stable (11 h) and para-derivative **1c** is the least stable (4 h). The maximum heat flow values follow the opposite pattern and decrease in a row **1c** > **1b** > **1a**. The results discussed are presented in Tables 3 and 4 and Figure 9.

The analysis of the kinetic data obtained at different temperatures followed by approximation with the Arrhenius equation allowed us to find the kinetic parameters of DS decomposition reactions occurring at 25 °C. The obtained results are presented in Table 5 and Figure 10. The

**Table 5. Calculated Kinetic Parameters of DS 1−3 Decomposition Reactions Occurring at 25 °C[a]**

| DS | $k_{298} \times 10^9$, $s^{-1}$ | $E_a$, kJ/mol |
|---|---|---|
| 2-$NO_2C_6H_4N_2^+TfO^-$ **1a** | 1.39 | 111.4 |
| 3-$NO_2C_6H_4N_2^+TfO^-$ **1b** | 2.90 | 159.7 |
| 4-$NO_2C_6H_4N_2^+TfO^-$ **1c** | 4.45 | 173.0 |
| 4-$MeOC_6H_4N_2^+TfO^-$ **1d** | 0.049 | 187.1 |
| 4-$NO_2C_6H_4N_2^+TsO^-$ **2** | 48.91 | 131.7 |
| 4-$NO_2C_6H_4N_2^+BF_4^-$ **3** | 18.75 | 140.3 |

[a] $k_{298}$—rate constant at 298 K; $E_a$—activation energy, kJ/mol.

arenediazonium triflates **1b−d** have higher activation energies comparing to tosylate **2** and tetrafluoroborate **3**. However, 2-nitrobenzenediazonium triflate is out of this line as it has the lowest activation energy among the DS studied.

Based on the approximation data, we have modeled the process of decomposition of the investigated DS over a large time period (Figures 11 and 12). According to the results, the stability of arenediazonium triflates depends on the substitution pattern. In particular, at 25 °C 3-nitrobenzenediazonium triflate has the longest half-life time of 83 years, whereas 2-nitrobenzenediazonium triflate has the shortest half-life time of 25 years (Figure 11). The nature of counterion affects greatly the DS stability (Figure 12). Thus, 4-nitrobenzenediazonium tosylate **2** and tetrafluoroborate **3** have close half-life times of 4.5 years, whereas 4-nitrobenzenediazonium triflate **1c** is much more stable with a half-life time of 46 years and a significantly lower maximum heat flow. Note that the effect of counterion on DS stability becomes noticeable only at low temperatures (25 °C), while at elevated temperatures (during

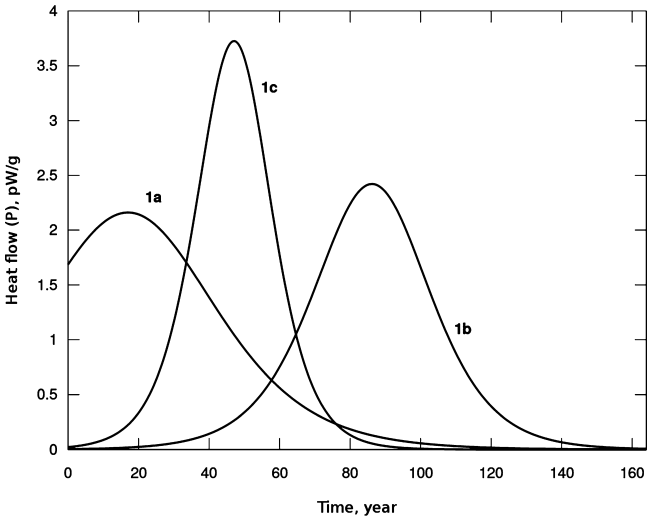


**Figure 11.** Heat flow ($P$) over the time dependency built upon modeling of the kinetic curves of the decomposition of 2-, 3- and 4-nitrobenzenediazonium triflates **1a−c** at 25 °C.

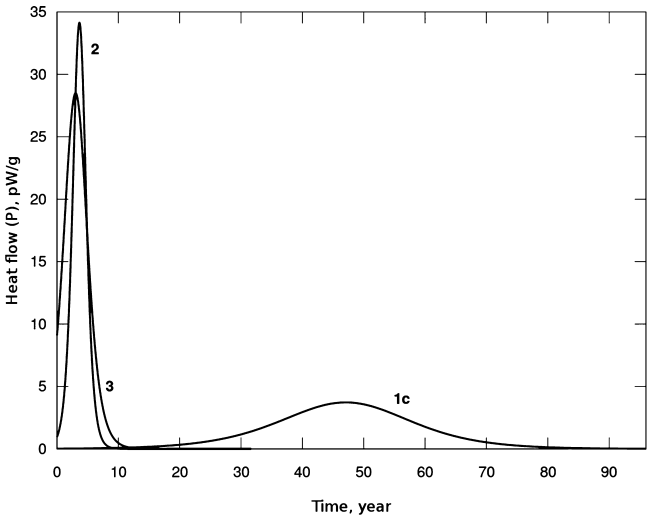


**Figure 12.** Heat flow ($P$) over the time dependency built upon modeling of the kinetic curves of the decomposition of 4-nitrobenzenediazonium tosulate **2**, triflate **1c**, and tetrafluoroborate **3** at 25 °C.

DSC/TGA or isothermal flow calorimetry at 75−85 °C) these differences disappear. This fact, as well as the values of activation energies, suggest that the stability of DS under normal storage conditions is largely determined by the strength of the crystal lattice. At higher temperatures, after the destruction of the crystal lattice, the speed and energy of the process are likely to be influenced by both the nature of the Ar−$N_2^+$ diazonium cation and the presence and nature of nucleophiles in the immediate environment.

Thus, considering all the data, we can draw several conclusions. First of all, DSC/TGA alone cannot serve as a reliable criterion for assessing the thermal stability and safety of DSs because in this case decomposition occurs at higher temperatures and is accompanied by intense evaporation of low-molecular-weight reaction products. In addition, during DSC/TGA analysis DSs decompose at different temperatures, which makes the analysis and comparison of the data complicated. Therefore, the study of DS thermal stability


DOI: 10.1021/acs.oprd.9b00307
Org. Process Res. Dev. XXXX, XXX, XXX−XXX

should be complemented by a more detailed investigation of the decomposition kinetics by isothermal flow calorimetry. The values of maximum heat flow, half-lives, and activation energies should be determined and approximation of the kinetics to normal conditions should be performed.

Second, the nature of counterion has a pronounced effect on DS stability. The approximation of experimental data with Arrhenius equation showed that arenediazonium triflates are the most stable during the storage, for example, 3-nitrobenzenediazonium triflate has a shelf-life of 83 years. Presumably, changing the counterion affects the probability of the occurrence of various mechanisms during the DS decomposition, which is discussed further and presented in Schemes 1 and 2.

**Scheme 1. Possible Mechanism of Thermal Decomposition of DSs 1b–d, 2, 3 (Nu = F, TsO, TfO)**

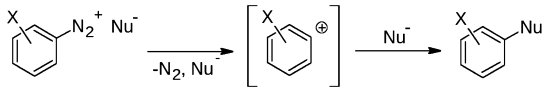


**Scheme 2. Possible Route of 1-Nitrocyclohexa-1,3-dien-5-yne [$C_6H_3NO_2$] ($\Delta m/z$ = 121.0) Formation (a) and Further Polymerization (b)**

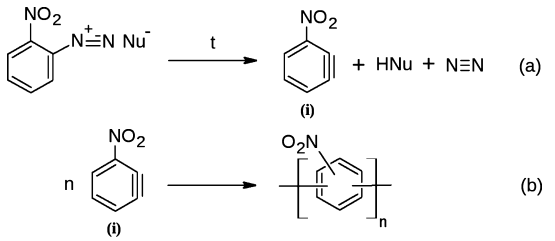


Finally, given the results of isothermal flow calorimetry, the DSs studied decompose with thermal effects close to the threshold value of 800 J/g for safe transportation, according to UNESCO.[6] Only in the case of 2-nitrobenzenediazonium triflate, the released energy of 1330 J/g exceeds the permissible value.

**GC–MS and LC–MS Study of Decomposition Products.** While it has long been established that the main products of the thermal decomposition of arenediazonium tetrafluoroborates are the corresponding aryl fluorides (the Balz–Schiemann reaction), the products of the thermolysis of arenediazonium triflates and tosylates remain unknown. We elucidated the structure of the compounds that appear after 14 days of decomposition of DSs **1–3** at 85 °C using GC–MS and LC–MS. To conduct the analysis, the unreacted DS was converted into corresponding aryl iodide by reaction with KI.

According to the GC–MS data (Supporting Information 2s, Figures S1–S11), the main products of the decomposition of DSs **1b**, **1c**, **1d** are the corresponding esters of nitro-phenyl trifluoromethanesulfonates ArOTf. The decomposition of arenediazoniumtosylate **2** resulted in the formation of nitrobenzene and 1-iodo-4-nitrobenzene (GC–MS). LC–MS ESI in the negative ionization mode also showed the presence of 4-nitrophenyl 4-methylbenzenesulfonate ester ($m/z$ = 292.1) among the decomposition products. In case of arenediazonium tetrafluoroborate **3**, the main decomposition product was the expected 1-fluoro-4-nitrobenzene. It should be noted that during the decomposition of all the DSs studied, significant amounts of resinous products that could not be elucidated by GC–MS were formed. Considering the GC–MS and LC–MS results, the following mechanism can be assumed for thermolysis of DSs **1b–d**, **2**, **3** (Scheme 1).

A completely different process takes place when 2-nitroarenediazonium triflate **1a** decomposes. In this case, the products of the diazonium group substitution by the triflate anion were not detected. The compounds formed during the DS **1a** decomposition were polymers. We were able to elucidate their structure by LC–MS (Table 6, MS spectra presented in Supporting Information 3s). The polymers found were suggested to be built upon the following repeating units: $NO_2C_6H_3$ ($\Delta m/z$ = 121.0) and [$NO_2C_6H_4SCF_3$] ($\Delta m/z$ = 223).

Apparently, the appearance of the abovementioned resinous compounds is associated with the polymerization processes as proven by the polymeric nature of products formed as a result of DS **1a** decomposition. We can infer that 1-nitrocyclohexa-1,3-dien-5-yne [$C_6H_3NO_2$] ($\Delta m/z$ = 121.0) is a monomer that is derived from DS according to the route (a) presented in Scheme 2.

**Table 6. Main Peaks Present on the LC–MS Chromatograms of the Decomposition Products of 2-Nitroarenediazonium Triflate 1a**

| ionization mode | $m/z$ | compound |
|---|---|---|
| positive ESI | 74.1; 297.1; 520.2; 743.2 | polymer chain P1 with the mass of repeating unit of 223, possibly, [$NO_2C_6H_4SCF_3$] |
| | 432.1; 553.1; 674.1; 795.1; 916.1; 1037.1; 1158.1 | polymer chain P2 with the mass of repeating unit of 121, [$C_6H_3NO_2$] |
| | 525.1; 646.1; 767.1; 888.1; 1009.1; 1130.1 | polymer chain P3 with the mass of repeating unit of 121, [$C_6H_3NO_2$]. The difference between P2 and P3 is 28, which corresponds to the nitrogen elimination |
| | 588.2; 710.1; 831.2; 952.2; 275.1; 785.8; 915.2; 1087.1 | polymer chain P4 with the mass of repeating unit of 121, [$C_6H_3NO_2$] |
| positive APCI | 394.0; 515.0; 635.9; 756.9; 877.8; 998.8; 1119.7 | polymer chain P5 with the mass of repeating unit of 121, [$C_6H_3NO_2$] |
| | 597.3; 875.4; 877.4; 879.4 | |
| negative ESI | 380.1; 501.1; 622.1; 743.1; 864.1 | polymer chain P6 with the mass of repeating unit of 121, [$C_6H_3NO_2$] |
| | 528.0; 649.1; 770.1; 891.1 | polymer chain P7 with the mass of repeating unit of 121, [$C_6H_3NO_2$] |
| | 149.0 | $TfO^-$ |
| | 276.8; 320.9; 436.7; 563.6; 936.2 | |


DOI: 10.1021/acs.oprd.9b00307
Org. Process Res. Dev. XXXX, XXX, XXX–XXX

The mechanism of further chain growth involving $C_6H_3NO_2$ as a monomer is ambiguous and requires special investigation lying beyond the scope of this work. However, based on the available data, we can assume the structure of the polymer formed as a result of the DS **1a** decomposition process (b) presented in Scheme 2. Previously, the appearance of polymer products during the thermal decomposition of *ortho*-carboxybenzenediazonium chloride was also explained by the intermediate formation of didehydrobenzene and naphthalene.[2h,i]

Importantly, the unique route found for DS **1a** decomposition including the formation of neutral $C_6H_3NO_2$ is consistent with the high instability of the intermediate involved in an alternative pathway (Scheme 1). Indeed, the 2-nitrobenzene-1-ylium cation that would be formed in this case is much less stable and energetically unfavorable comparing to aryl cations derived from the other DSs because of the fact that the electron-withdrawing group $NO_2$ is next to the carbocationic center.

**Quantum Chemical Calculations.** Given the identified products of DS **1a**−**c**, **2**, **3** thermal decomposition, we for the first time predicted the thermodynamics of the occurring processes using DFT calculations at the RB3LYP/aug-cc-pVDZ level of theory. We have optimized geometry of DS **1a**−**c**, **2**, **3** and diazonium group substitution products. The nature of located stationary points was confirmed by the absence of imaginary frequencies in the IR spectrum. Cartesian coordinates of all compounds and calculated thermodynamic parameters are given in Supporting Information 4s. We have explored esters and substituted phenols as the major products of triflates **1a**−**c** and tosylate **2** decomposition and 4-fluoronitrobenzene as the major product of tetrafluoroborate **3** decomposition. The predicted and experimental thermodynamic parameters of the reactions are presented in Tables 7 and 8. Considering DSC/TGA results that showed that thermolysis of tetrafluoroborate **3** initially causes $BF_3$ detachment with the formation of 4-$NO_2C_6H_4N_2^+F^-$ **3a** (Scheme 1), we calculated the thermodynamics of this reaction along with other possible routes (Table 6, entries 6a, b).

**Table 7. Predicted Thermodynamic Parameters of DS 1a−c, 2, 3 Decomposition Reactions According to Quantum Chemical Calculations at the RB3LYP/aug-cc-pVDZ Level of Theory**

| entry | reaction | $\Delta G_{298}$, kJ/mol | $\Delta H_{298}$, kJ/mol | $\Delta S^{*}_{298.15}$, kJ/mol |
|---|---|---|---|---|
| 1 | 2-$NO_2C_6H_4N_2^{+\cdot}OTf \rightarrow$ 2-$NO_2C_6H_4OTf + N_2$ | −268.6 | −230.1 | 38.5 |
| 2 | 3-$NO_2C_6H_4N_2^{+\cdot}OTf \rightarrow$ 3-$NO_2C_6H_4OTf + N_2$ | −282.4 | −242.8 | 39.6 |
| 3 | 4-$NO_2C_6H_4N_2^{+\cdot}OTf \rightarrow$ 4-$NO_2C_6H_4OTf + N_2$ | −287.6 | −248.0 | 39.6 |
| 4 | 4-$MeOC_6H_4N_2^{+\cdot}OTf \rightarrow$ 4-$MeOC_6H_4OTf + N_2$ | −238.1 | −200.5 | 37.7 |
| 5 | 4-$NO_2C_6H_4N_2^{+\cdot}OTs \rightarrow$ 4-$NO_2C_6H_4OTs + N_2$ | −328.4 | −283.9 | 44.6 |
| 6 | 4-$NO_2C_6H_4N_2^{+\cdot}BF_4 \rightarrow$ 4-$NO_2C_6H_4F + BF_3 + N_2$ | −276.2 | −188.4 | 87.9 |
| 6a | 4-$NO_2C_6H_4N_2^{+\cdot}BF_4 \rightarrow$ 4-$NO_2C_6H_4N_2F + BF_3$ | 76.2 | 124.6 | 48.5 |
| 6b | 4-$NO_2C_6H_4N_2F^- \rightarrow$ 4-$NO_2C_6H_4F + N_2$ | −352.3 | −312.9 | 39.4 |

Overall, for all reactions of DS **1b**−**d**, **2**, and **3** decomposition the calculated enthalpy values are consistent with the experimental ones obtained by isothermal flow calorimetry. Therefore, the suggested reactions make the main contribution to the energy of DS exothermic decomposition (Tables 6 and 7). The obtained results prove that DFT calculations at the RB3LYP/aug-cc-pVDZ level of theory are a convenient and fairly precise method for theoretical estimation of the thermal effects of DS decomposition. A single case, where we had significant deviation between the data of isothermal flow calorimetry and calculation results is 2-nitroarenediazonium triflate **1a** (Table 7). However, this is consistent with GC−MS and LC−MS data demonstrating that decomposition of DS **1a** proceeds via different route (Scheme 2) and does not result in 2-$NO_2C_6H_4OTf$.

In some cases, the enthalpy values of DS **1**−**3** exothermic decomposition measured by DSC/TGA were found to be significantly less than both predicted ones and values obtained by isothermal flow calorimetry (Table 8). It can be explained by the fact that decomposition of DSs during DSC/TGA analysis occurs at temperatures much higher than 85 °C (Table 2), resulting in an evaporation process, accompanied by a significant weight loss, which reduces the thermal effect of the reaction.

Importantly, the DFT calculations were carried out assuming reagents and products are isolated molecules, therefore, the electric field of the crystal was neglected. However, the very fact that the predicted energies are in good agreement with the experimental values measured by flow calorimetry for the decomposition reactions of five DSs with different counterions and ring substituents **1b**−**d**, **2**, and **3** (Table 8) indicates that the major contribution to the reaction thermodynamics is made by the chemical transformations, whereas the effects of changing the crystal lattices are minor. Possibly, it is because of the fact that both reagents and products remain solid (except $N_2$), thus, there is a compensation for the thermal effects of the transformation of the crystal lattices of the starting materials and products. From an application prospective, it is also important that the proposed quantum-chemical approach to assessing the thermodynamics of decomposition reactions of DSs is relatively easy to implement. While calculations that take into account unknown transformations of the crystal lattice are much more laborious, sophisticated, and cannot yet be widely used to predict the thermal effects of chemical reactions, despite the known progress in calculating the crystalline state of benzenediazonium chloride and tetrafluoroborate.[2c,d]

## CONCLUSIONS

In conclusion, for the first time we have determined the thermodynamics and kinetics of thermal decomposition of a series of aromatic DSs $ArN_2^+ X^-$ with various counterions X = TfO, TsO, $BF_4$ by isothermal flow calorimetry and provided the quantitative assessment of the storage stability of solid DSs under normal conditions. Additionally, we have established how the aromatic substitution pattern in diazonium cation and the nature of the counterion affect the processes occurring during the thermolysis of DSs studied.

We demonstrated that thermodynamic parameters of DS thermal decomposition reactions calculated by DFT at RB3LYP/aug-cc-pVDZ consisted experimental data obtained by isothermal flow calorimetry for all 3- and 4-substituted DSs investigated (**1b**−**d**, **2**, **3**). For these DSs, the main


DOI: 10.1021/acs.oprd.9b00307
Org. Process Res. Dev. XXXX, XXX, XXX−XXX

Table 8. Experimental and Predicted Enthalpies of Decomposition of Diazonium Salts (RB3LYP/aug-cc-pVDZ)

| | predicted enthalpy | experimental enthalpy (flow calorimetry) | | | DSC/TGA |
|---|---|---|---|---|---|
| reaction | $\Delta H_{298}$, ($\Delta H_{353}$) kJ/mol | $\Delta H_{348}$, kJ/mol | $\Delta H_{353}$, kJ/mol | $\Delta H_{358}$, kJ/mol | $\Delta H$, kJ/mol |
| $2\text{-}NO_2C_6H_4N_2^+Tf^- \rightarrow 2\text{-}NO_2C_6H_4OTf + N_2$ | −230 (−230.4) | −414 | −386 | −396 | −203.4 |
| $3\text{-}NO_2C_6H_4N_2^+TfO^- \rightarrow 3\text{-}NO_2\text{-}C_6H_4OTf + N_2$ | −243 (−243.2) | −228 | −230 | −225 | −238.5 |
| $4\text{-}NO_2C_6H_4N_2^+TfO^- \rightarrow 4\text{-}NO_2\text{-}C_6H_4OTf + N_2$ | −248 (−248.4) | −200 | −235 | −250 | −65.8 |
| $4\text{-}MeOC_6H_4N_2^+TfO^- \rightarrow 4\text{-}MeOC_6H_4OTf + N_2$ | −201 (−200.8) | −183 | −183 | −106 | −64.5 |
| $4\text{-}NO_2C_6H_4N_2^+TfO^- \rightarrow 4\text{-}NO_2C_6H_4OTs + N_2$ | −284 (−284.0) | −253 | −232 | −231 | −117.3 |
| $4\text{-}NO_2C_6H_4N_2^+BF_4^- \rightarrow 4\text{-}NO_2C_6H_4F + BF_3 + N_2$ | −188 (−189.5) | −173 | −156 | −147 | −54.3 |

decomposition route is the elimination of nitrogen with the formation of benzene-1-ylium ions that subsequently react with the corresponding anions. A completely different process occurs during the thermolysis of 2-nitrobenzene diazonium triflate **1a**. In this case, the polymeric products are formed, probably through the primary generation of 1-nitrocyclohexa-1,3-dien-5-yne.

## ■ ASSOCIATED CONTENT

### Supporting Information

The Supporting Information is available free of charge on the ACS Publications website at DOI: 10.1021/acs.oprd.9b00307.

Results of modeling and deconvolution of heat flow experimental kinetic curves acquired in isothermal conditions as well as results of quantum chemical calculations (PDF)

Details of Diazo-Flow-Calorimetry; LC-MS; and Quantum chemical calculations (ZIP)

## ■ AUTHOR INFORMATION


### Corresponding Authors

*E-mail: Alexander.A.Bondarev@gmail.com (A.A.B.).

*E-mail: filimonov@tpu.ru (V.D.F.).

### ORCID

Ksenia S. Stankevich: 0000-0002-6701-7582

Victor D. Filimonov: 0000-0003-4729-8871


### Author Contributions

The manuscript was written through contributions of all authors. All authors have given approval to the final version of the manuscript.

### Notes

The authors declare no competing financial interest.

## ■ ACKNOWLEDGMENTS

The research was funded by RFBR grant 17-03-01097.

## ■ ABBREVIATIONS

DSs, diazonium salts; ADTs, arenediazonium tosylates; ADTfs, arenediazonium trifluoromethane sulfonates; DSC/TGA, differential scanning calorimetry and thermal gravimetric analysis; UNECE, United Nations Economic Commission for Europe; GC−MS, gas chromatography−mass spectrometry; LC−MS, liquid chromatography−mass spectrometry; ESI, electrospray ionization source; APCI, atmospheric pressure chemical ionization source; DFT, density functional theory

## ■ REFERENCES


(1) (a) Zollinger, H. *Diazo Chemistry I: Aromatic and Heteroaromatic Compounds*; VCH: Weinheim, 1994. (b) Roglans, A.; Pla-Quintana, A.; Moreno-Mañas, M. Diazonium Salts as Substrates in Palladium-Catalyzed Cross-Coupling Reactions. *Chem. Rev.* **2006**, *106*, 4622−4643. (c) Bonin, H.; Fouquet, E.; Felpin, F.-X. Aryl Diazonium versus Iodonium Salts: Preparation, Applications and Mechanisms for the Suzuki-Miyaura Cross-Coupling Reaction. *Adv. Synth. Catal.* **2011**, *353*, 3063−3084. (d) Mo, F.; Dong, G.; Zhang, Y.; Wang, J. Recent Applications of Arene Diazonium Salts in Organic Synthesis. *Org. Biomol. Chem.* **2013**, *11*, 1582. (e) Kölmel, D. K.; Jung, N.; Bräse, S. Azides − Diazonium Ions − Triazenes: Versatile Nitrogen-Rich Functional Groups. *Aust. J. Chem.* **2014**, *67*, 328. (f) Deadman, B. J.; Collins, S. G.; Maguire, A. R. Taming Hazardous Chemistry in Flow: The Continuous Processing of Diazo and Diazonium Compounds. *Chem.—Eur. J.* **2014**, *21*, 2298−2308. (g) Idowu, O. S.; Kolawole, A. O.; Abegoke, O. A.; Kolade, Y. T.; Fasanmade, A. A.; Olaniyi, A. A. *J. AOAC Int.* **2005**, *88*, 1108−1113.

(2) (a) Mahouche-Chergui, S.; Gam-Derouich, S.; Mangeney, C.; Chehimi, M. M. Aryl Diazonium Salts: A New Class of Coupling Agents for Bonding Polymers, Biomacromolecules and Nanoparticles to Surfaces. *Chem. Soc. Rev.* **2011**, *40*, 4143. (b) Sheng, M.; Frurip, D.; Gorman, D. Reactive Chemical Hazards of Diazonium Salts. *J. Loss Prev. Process Ind.* **2015**, *38*, 114−118. (c) Bondarchuk, S. V. Impact Sensitivity of Crystalline Phenyl Diazonium Salts: A First-Principles Study of Solid-State Properties Determining the Phenomenon. *Int. J. Quantum Chem.* **2017**, *117*, No. e25430. (d) Bondarchuk, S. V. Impact Sensitivity of Aryl Diazonium Chlorides: Limitations of Molecular and Solid-State Approach. *J. Mol. Graphics Modell.* **2019**, *89*, 114−121. (e) Bräse, S.; Dahmen, S.; Popescu, C.; Schroen, M.; Wortmann, F.-J. The Structural Influence in the Stability of Polymer-Bound Diazonium Salts. *Chem.—Eur. J.* **2004**, *10*, 5285−5296. (f) Thon, D.; Fürst, M. C. D.; Altmann, L.-M.; Heinrich, M. R. Frozen Aryldiazonium Chlorides in Radical Reactions with Alkenes and Arenes. *Tetrahedron* **2018**, *74*, 5289−5294. (g) Oger, N.; Le Grognec, E.; Felpin, F.-X. Handling Diazonium Salts in Flow for Organic and Material Chemistry. *Org. Chem. Front.* **2015**, *2*, 590−614. (h) de Rossi, R. H.; Bertorello, H. E.; Rossi, R. A. Thermal Decomposition Reactions of Carboxybenzenediazonium Salts. I. 1,4-Dehydroaromatic Compounds from O-Carboxybenzenediazonium Salts. *J. Org. Chem.* **1970**, *35*, 3328−3332. (i) Bertorello, H. E.; Rossi, R. A.; Hoyos de Rossi, R. Thermal Decomposition of Carboxybenzenediazonium Salts. II. 1,3-Dehydroaromatic Compounds from Carboxybenzenediazonium Salts. *J. Org. Chem.* **1970**, *35*, 3332−3338.

(3) (a) Filimonov, V. D.; Trusova, M.; Postnikov, P.; Krasnokutskaya, E. A.; Lee, Y. M.; Hwang, H. Y.; Kim, H.; Chi, K.-W. Unusually Stable, Versatile, and Pure Arenediazonium Tosylates: Their Preparation, Structures, and Synthetic Applicability. *Org. Lett.* **2008**, *10*, 3961−3964. (b) Filimonov, V. D.; Krasnokutskaya, E. A.; Kassanova, A. Z.; Fedorova, V. A.; Stankevich, K. S.; Naumov, N. G.; Bondarev, A. A.; Kataeva, V. A. Synthesis, Structure, and Synthetic Potential of Arenediazonium Trifluoromethanesulfonates as Stable and Safe Diazonium Salts. *Eur. J. Org. Chem.* **2018**, *2019*, 665−674.

(4) (a) Krasnokutskaya, E.; Semenischeva, N.; Filimonov, V.; Knochel, P. A New, One-Step, Effective Protocol for the Iodination of Aromatic and Heterocyclic Compounds via Aprotic Diazotization of Amines. *Synthesis* **2007**, *2007*, 81−84. (b) Filimonov, V.; Chi, K.-W.; Semenischeva, N.; Krasnokutskaya, E.; Tretyakov, A.; Hwang, H. Sulfonic Acid Based Cation-Exchange Resin: A Novel Proton Source for One-Pot Diazotization-Iodination of Aromatic Amines in Water. *Synthesis* **2008**, *2008*, 185−187. (c) Gorlushko, D. A.; Filimonov, V.




DOI: 10.1021/acs.oprd.9b00307
Org. Process Res. Dev. XXXX, XXX, XXX−XXX

D.; Krasnokutskaya, E. A.; Semenischeva, N. I.; Go, B. S.; Hwang, H. Y.; Cha, E. H.; Chi, K.-W. Iodination of Aryl Amines in a Water-Paste Form via Stable Aryl Diazonium Tosylates. *Tetrahedron Lett.* **2008**, *49*, 1080−1082. (d) Lee, Y. M.; Moon, M. E.; Vajpayee, V.; Filimonov, V. D.; Chi, K.-W. Efficient and Economic Halogenation of Aryl Amines via Arenediazonium Tosylate Salts. *Tetrahedron* **2010**, *66*, 7418−7422. (e) Moon, M. E.; Choi, Y.; Lee, Y. M.; Vajpayee, V.; Trusova, M.; Filimonov, V. D.; Chi, K.-W. An Expeditious and Environmentally Benign Preparation of Aryl Halides from Aryl Amines by Solvent-Free Grinding. *Tetrahedron Lett.* **2010**, *51*, 6769−6771. (f) Chi, K.-W.; Filimonov, V.; Trusova, M.; Krasnokutskaya, E.; Postnikov, P.; Choi, Y. A Green Procedure for the Diazotization-Iodination of Aromatic Amines under Aqueous, Strong-Acid-Free Conditions. *Synthesis* **2011**, *2011*, 2154−2158. (g) Filimonov, V.; Parello, J.; Kutonova, K.; Trusova, M.; Postnikov, P. A Simple and Effective Synthesis of Aryl Azides via Arenediazonium Tosylates. *Synthesis* **2013**, *45*, 2706−2710. (h) Kutonova, K. V.; Trusova, M. E.; Stankevich, A. V.; Postnikov, P. S.; Filimonov, V. D. Matsuda−Heck Reaction with Arenediazonium Tosylates in Water. *Beilstein J. Org. Chem.* **2015**, *11*, 358−362. (i) Postnikov, P.; Bräse, S.; Kutonova, K.; Jung, N.; Trusova, M.; Filimonov, V. Arenediazonium Tosylates (ADTs) as Efficient Reagents for Suzuki−Miyaura Cross-Coupling in Neat Water. *Synthesis* **2016**, *49*, 1680−1688. (j) Vajpayee, V.; Song, Y. H.; Ahn, J.-S.; Chi, K.-W. One-Pot Homo- and Cross-Coupling Reactions of Arenediazonium Tosylate Salts for the Synthesis of Biaryls and Polyaryls. *Bull. Korean Chem. Soc.* **2011**, *32*, 2970−2972.

(5) (a) Riss, P. J.; Kuschel, S.; Aigbirhio, F. I. No Carrier-Added Nucleophilic Aromatic Radiofluorination Using Solid Phase Supported Arenediazonium Sulfonates and 1-(Aryldiazenyl)piperazines. *Tetrahedron Lett.* **2012**, *53*, 1717−1719. (b) Velikorodov, A. V.; Ionova, V. A.; Temirbulatova, S. I.; Suvorova, M. A. Some Chemical Transformations of Alkyl (4-Aminophenyl)carbamates. *Russ. J. Org. Chem.* **2013**, *49*, 1004−1009. (c) Wang, W.; Tang, Z.; Zhang, Y.; Wang, T. Rhodium(I)-Catalyzed Synthesis of Aryltriethoxysilanes from Arenediazonium Tosylate Salts with Triethoxysilane. *Synlett* **2010**, *2010*, 804−808. (d) Postnikov, P. S.; Trusova, M. E.; Fedushchak, T. A.; Uimin, M. A.; Ermakov, A. E.; Filimonov, V. D. Aryldiazonium Tosylates as New Efficient Agents for Covalent Grafting of Aromatic Groups on Carbon Coatings of Metal Nanoparticles. *Nanotechnol. Russ.* **2010**, *5*, 446−449. (e) Min, M.; Seo, S.; Lee, J.; Lee, S. M.; Hwang, E.; Lee, H. Changes in Major Charge Transport by Molecular Spatial Orientation in Graphene Channel Field Effect Transistors. *Chem. Commun.* **2013**, *49*, 6289.

(6) http://www.unece.org/trans/danger/danger.html.

(7) (a) Ullrich, R.; Grewer, T. Decomposition of Aromatic Diazonium Compounds. *Thermochim. Acta* **1993**, *225*, 201−211. (b) Brown, L. L.; Drury, J. S. Nitrogen Isotope Effects in the Decomposition of Diazonium Salts. *J. Chem. Phys.* **1965**, *43*, 1688−1691. (c) Storey, P. D. Calorimetric Studies of the Thermal Explosion Properties of Aromatic Diazonium Salts. *Institution of Chemical Engineers Symposium Series*, 1981; Vol. *68*, p 71

(8) (a) Ticmanis, U.; Wilker, S.; Pantel, G.; Guillaume, P.; Balès, C.; van der Meer, N. Principles of a STANAG for the Estimation of the Chemical Stability of Propellants by Heat Flow Calorimetry. *Proceedings of International Annual Conference Institut Chemische Technologie*, 2000; Vol. *31*, p 2. (b) Guillaume, P.; Rat, M.; Wilker, S.; Pantel, G. Microcalorimetric and Chemical Studies of Propellants. *Proceedings of International Annual Conference Institut Chemische Technologie*, 1998; Vol. *29*, p 133. (c) STANAG 4582. *Explosives, Nitrocellulose Based Propellants—Stability Test Procedures and Requirements Using HFC Brussels: North Atlantic Treaty Organization*; Military Agency for Standardization, 2004. (d) Jelisavac, L.; Stojiljković, S.; Gačić, S.; Brzić, S.; Bobić, N. Comparative Examination of the Chemical Stability of Powders and Double − Base Rocket Propellants by Measuring Heat Activities and Stabilizer Content. *Sci.-Tech. Rev.* **2014**, *64*, 48−54.

(9) (a) Williams, T.; Kelley, C. Gnuplot 4.5: An Interactive Plotting Program. http://gnuplot.info (accessed June 7, 2011). (b) R Core Team. *R: A Language and Environment for Statistical Computing*; R Foundation for Statistical/Computing: Vienna, Austria, 2017. https://www.R-project.org/.

(10) Sturm, M.; Bertsch, A.; Gröpl, C.; Hildebrandt, A.; Hussong, R.; Lange, E.; Pfeifer, N.; Schulz-Trieglaff, O.; Zerck, A.; Reinert, K.; et al. OpenMS − An Open-Source Software Framework for Mass Spectrometry. *BMC Bioinf.* **2008**, *9*, 163.

(11) Frisch, M. J.; Trucks, G. W.; Schlegel, H. B.; Scuseria, G. E.; Robb, M. A.; Cheeseman, J. R.; Scalmani, G.; Barone, V.; Petersson, G. A.; Nakatsuji, H.; Li, X.; Caricato, M.; Marenich, A.; Bloino, J.; Janesko, B. G.; Gomperts, R.; Mennucci, B.; Hratchian, H. P.; Ortiz, J. V.; Izmaylov, A. F.; Sonnenberg, J. L.; Williams-Young, D.; Ding, F.; Lipparini, F.; Egidi, F.; Goings, J.; Peng, B.; Petrone, A.; Henderson, T.; Ranasinghe, D.; Zakrzewski, V. G.; Gao, J.; Rega, N.; Zheng, G.; Liang, W.; Hada, M.; Ehara, M.; Toyota, K.; Fukuda, R.; Hasegawa, J.; Ishida, M.; Nakajima, T.; Honda, Y.; Kitao, O.; Nakai, H.; Vreven, T.; Throssell, K.; Montgomery, J. A., Jr.; Peralta, J. E.; Ogliaro, F.; Bearpark, M.; Heyd, J. J.; Brothers, E.; Kudin, K. N.; Staroverov, V. N.; Keith, T.; Kobayashi, R.; Normand, J.; Raghavachari, K.; Rendell, A.; Burant, J. C.; Iyengar, S. S.; Tomasi, J.; Cossi, M.; Millam, J. M.; Klene, M.; Adamo, C.; Cammi, R.; Ochterski, J. W.; Martin, R. L.; Morokuma, K.; Farkas, O.; Foresman, J. B.; Fox, D. J. *Gaussian 09*, Revision A.02; Gaussian, Inc.: Wallingford CT, 2016.

(12) Koval'chuk, E. P.; Reshetnyak, O. V.; Kozlovs'ka, Z. Y.; Błażejowski, J.; Gladyshevs'kyj, R. Y.; Obushak, M. D. Mechanism of the Benzenediazonium Tetrafluoroborate Thermolysis in the Solid State. *Thermochim. Acta* **2006**, *444*, 1−5.

(13) Cai, J.; Liu, R. Kinetic Analysis of Solid-State Reactions: A General Empirical Kinetic Model. *Ind. Eng. Chem. Res.* **2009**, *48*, 3249−3253.

(14) (a) Bondarchuk, S. V.; Minaev, B. F. Density Functional Study of Ortho-Substituted Phenyl Cations in Polar Medium and in the Gas Phase. *Chem. Phys.* **2011**, *389*, 68−74. (b) Bondarchuk, S. V.; Minaev, B. F. State-Dependent Global and Local Electrophilicity of the Aryl Cations. *J. Phys. Chem. A* **2014**, *118*, 3201−3210.



DOI: 10.1021/acs.oprd.9b00307
*Org. Process Res. Dev.* XXXX, XXX, XXX−XXX